



Cite this: *Chem. Commun.*, 2015, 51, 15469

Received 2nd July 2015,  
Accepted 3rd September 2015

DOI: 10.1039/c5cc05446j

www.rsc.org/chemcomm

# $\text{Na}_2\text{MoO}_{2-\delta}\text{F}_{4+\delta}$ – a perovskite with a unique combination of atomic orderings and octahedral tilts†

Hajime Ishikawa,‡<sup>a</sup> Irene Munaò,‡<sup>b</sup> Bela E. Bode,<sup>b</sup> Zenji Hiroi<sup>a</sup> and Philip Lightfoot\*<sup>b</sup>

$\text{Na}_2\text{MoO}_{2-\delta}\text{F}_{4+\delta}$  ( $\delta \sim 0.08$ ) displays a unique variant of the perovskite structure, with simultaneous (Na,vacancy) ordering on the A-site, (Na,Mo) ordering on the B-site, (O,F) ordering on the anion site and an unusual  $\text{NaNbO}_3$ -like octahedral tilt system.

The perovskite structure is the most ubiquitous and important in solid state chemistry. Its significance to functional materials lies, to a large extent, in the degree of compositional and structural flexibility available, starting from the aristotype cubic  $\text{ABX}_3$  structure. Thus, it is possible to incorporate a vast range of substitutions at the A and B cation sites and the X anion site, including mixed ion species and also vacancies at each site. If there is a sufficient chemical driving force, the species (atoms or vacancies) at the A, B and X sites may be crystallographically ordered, and it is this ordering that gives much of the richness to perovskite chemistry.<sup>1,2</sup> The second common structural feature of perovskites is ‘tilting’ of the  $\text{BX}_6$  octahedral units, and the nature of the common tilting schemes is well understood.<sup>3–5</sup> This paper describes a unique variant of the perovskite structure,  $\text{Na}_2\text{MoO}_{2-\delta}\text{F}_{4+\delta}$  ( $\delta \sim 0.08$ ) which displays simultaneous atomic order at all three sites, A, B and X, together with an unusual octahedral tilt scheme.

$\text{Na}_2\text{MoO}_{2-\delta}\text{F}_{4+\delta}$  was prepared by hydrothermal reaction of a mixture of NaF (1 mmol),  $\text{MoO}_3$  (1 mmol),  $\text{MoO}_2$  (1 mmol), guanidinium carbonate (1 mmol),  $\text{H}_2\text{O}$  (0.2 ml) and HF (48% aq.; 0.2 ml). This mixture was sealed in a Teflon-lined stainless steel autoclave and heated to 160 °C for 3 days. Blue air-stable crystals were recovered by filtration. Powder X-ray diffraction suggested the product to contain a small amount of residual  $\text{MoO}_2$ , which appears as a black powder on the surface of some crystals. Guanidine is not incorporated into the product, but attempts to prepare this phase from similar reactions, omitting the guanidinium carbonate, failed to produce the same

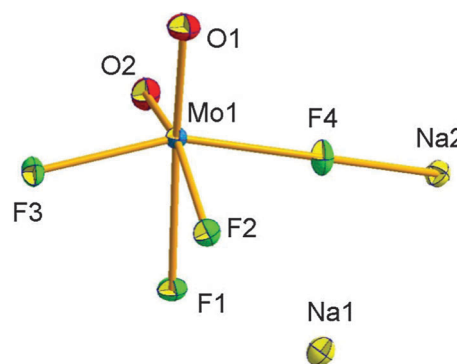


Fig. 1 Asymmetric unit of  $\text{Na}_2\text{MoO}_{2-\delta}\text{F}_{4+\delta}$ . Bond lengths (Å) around Mo are: Mo–O(1) 1.6837(15), Mo–O(2) 1.7273(14), Mo–F(1) 2.1212(11), Mo–F(2) 2.0499(12), Mo–F(3) 1.9599(18), Mo–F(4) 1.916(2).

product. The crystal structure was analysed using single crystal X-ray diffraction (see ESI†). The asymmetric unit (Fig. 1) contains one  $\text{Na}_2\text{MoO}_{2-\delta}\text{F}_{4+\delta}$  formula unit and, in particular, incorporates two distinct Na sites. Further inspection reveals that the structure is a unique variant of perovskite, incorporating Na on both the A and B sites, with fully ordered (Na,vacancy) on the A-site, fully ordered (Na,Mo) on the B-site and (O,F) fully ordered (within the constraints of stoichiometry – see later) on the X-site (Fig. 2). In addition there are octahedral tilts around each of the principal pseudo-cubic axes. This unprecedented atomic ordering and tilt scheme gives rise to a large, low-symmetry unit cell, of dimensions approximately  $\sqrt{2}a_p \times \sqrt{2}a_p \times 4a_p$  (where  $a_p$  is the cubic aristotype unit cell parameter)§.

The cation ordering scheme (Fig. 2) has an alternating ‘rock-salt’ like arrangement of Na(2) and Mo on the B-sites and a layered ordering of Na(1) and vacancies on the A-site. Rock-salt ordering on the B-site is relatively common in oxide perovskites, being driven by a large size/charge difference of the two B-site cations.<sup>2</sup> This is the situation in the present case. A-site ordering is relatively rare,<sup>2</sup> but ordering of cations and vacancies does occur in compounds such as  $\text{La}_{1/3}\text{NbO}_3$ , where a layered ordering of vacancies and 2/3 occupied La sites exists.<sup>6</sup> This type of ordering is facilitated by the tendency of the d<sup>0</sup> cation at the B-site to undergo a 2nd-order Jahn–Teller off-centring

<sup>a</sup> Institute for Solid State Physics, University of Tokyo, Kashiwa 277-8581, Japan

<sup>b</sup> School of Chemistry and EaStChem, University of St Andrews, St Andrews, Fife, KY16 9ST, UK. E-mail: pl@st-and.ac.uk

† Electronic supplementary information (ESI) available: Bond valence sums, single crystal and powder XRD, distortion mode analysis, crystallographic data (CIF). CIF data have been deposited with ICSD: deposition number CSD 429840. See DOI: 10.1039/c5cc05446j

‡ These authors contributed equally to this work.



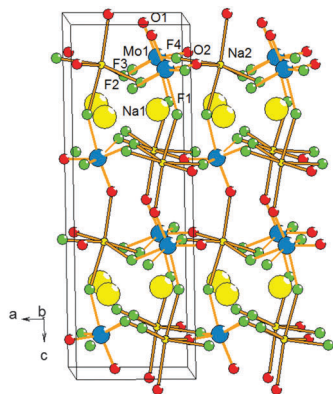


Fig. 2 Unit cell packing; note the details of the atomic ordering at A, B and X sites.

to alleviate bond strains,<sup>2</sup> such that the single, short Nb–O bond correlates with the A-site vacancy layer. This situation is not so simple in the present case, due to the presence of two short Mo–O bonds, and also the O/F ordering. The long-range nature of the anion ordering here must therefore be considered as correlated with the A-site ordering.

The Mo site in  $\text{Na}_2\text{MoO}_{2-\delta}\text{F}_{4+\delta}$  (Fig. 1) exhibits two short Mo–O bonds in a *cis* configuration. A locally *cis* configuration is normal in Mo oxyfluorides,<sup>7</sup> and many early transition metal oxyfluorides do retain long-range ordering of O/F ligands.<sup>8,9</sup> However, long-range ordering of O/F is less common in many  $d^0$  cation oxyfluorides with perovskite-related structures.<sup>10</sup> Indeed, the closest compositional analogue of the title compound,  $\text{KNaMoO}_2\text{F}_4$  has a related structure, displaying a similar type of A and B cation ordering, but shows ordering of only one of the oxide ligands, with the other being disordered amongst the four possible *cis* positions.<sup>11</sup>

Another feature of the  $\text{Na}_2\text{MoO}_{2-\delta}\text{F}_{4+\delta}$  structure, which might seem surprising at first sight, is the ordering of predominantly oxide (O(1)) rather than fluoride (F(1)) ligands within the A-site vacancy layers (Fig. 3(b)). Hence, the seven shortest bonds (2.30–2.56 Å) around the Na(1) site are all Na–F bonds, with the nearest Na–O contact being 2.72 Å (Fig. 3(a)). Association of Na–F seems reasonable on the basis of ‘hard’–‘hard’ interactions, but Na···O avoidance might seem less satisfactory based on bond valence considerations. Despite this apparent ‘underbonding’ around O(1), however, a full bond-valence sum (BVS) analysis (see ESI† for further details) does show the bonding around each atom is well satisfied: BVS values (valence units) are Mo(1): 5.83, Na(1) 1.10, Na(2) 1.22, O(1) 2.05, O(2) 1.94, F(1) 0.96,

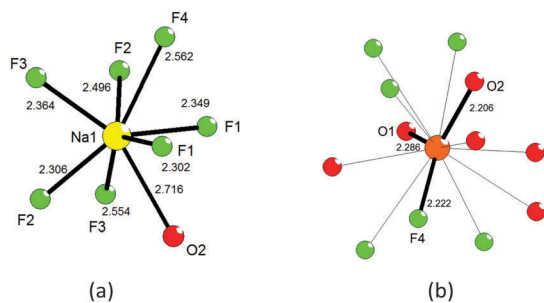


Fig. 3 Local coordination around the A-sites (a) Na(1): 4 + 4 coordination due to in-phase local tilts (b) vacancy site: 3 + 6 coordination due to out-of-phase local tilts.

F(2) 1.04, F(3) 1.10, F(4) 1.06. This situation parallels that seen in  $\text{La}_{1/3}\text{NbO}_3$ , where the A-site vacancies associate with the more covalently bonded anions. At this stage the single crystal structure has been refined as stoichiometric “ $\text{Na}_2\text{MoO}_2\text{F}_4$ ” and both the refined structure and the BVS analysis appear compatible with the Mo occurring purely as oxidation state VI. This is also supported by comparisons to closely related structures and compositions such as  $\text{KNaMoO}_2\text{F}_4$  and  $\text{Na}_2\text{MoO}_2\text{F}_4 \cdot \text{H}_2\text{O}$ .<sup>12</sup> In the latter compound, which has an unusual layered perovskite-related structure, the Mo–X bond lengths (Å) are Mo–O: 1.685, 1.706, Mo–F(eq.): 2.064, 2.126, Mo–F(ax.): 1.928, 1.963, in excellent agreement with those reported here. However, the observation of an intense blue colour for the title compound is curious, whereas both  $\text{KNaMoO}_2\text{F}_4$  and  $\text{Na}_2\text{MoO}_2\text{F}_4 \cdot \text{H}_2\text{O}$  are colourless. The colour is most likely due to a slight reduction to  $\text{Mo}^{5+}$ . In order to probe this possibility further we carried out both EPR and magnetisation measurements in order to directly probe the Mo oxidation state. Unfortunately direct chemical analysis for O/F content or red-ox activity was precluded by the presence of small amounts of extraneous  $\text{MoO}_2$ . The magnetisation data and EPR spectrum are provided in ESI†. The derived magnetic moment from magnetic susceptibility is consistent with a  $\text{Mo}^{5+}$  content of 8% of the total Mo. Several possible models of off-stoichiometry, in order to account for the observed reduction, were tested; these are discussed in the ESI†, with the most plausible being a minor F occupancy at the two O sites, consistent with a value  $\delta \sim 0.08$  in the formula  $\text{Na}_2\text{MoO}_{2-\delta}\text{F}_{4+\delta}$ .

Fig. 2 shows octahedral tilting around the *b*-axis of the monoclinic unit cell; this corresponds to simultaneous and equivalent ‘out-of-phase’ tilts around the *a* and *b* axes of the parent cubic cell. The tilting around the *c*-axis is, however, more unusual and does not correspond to one of the simple Glazer tilt systems.<sup>3,5</sup> Fig. 4 and 5 show that the ‘quadrupling’ of the unit cell along *c* is due to a more complex tilt around *c*, such that there are successively ‘in-phase’, ‘out-of-phase’, ‘in-phase’ tilt relations along this direction or, alternatively, the tilt sequence can be described as ‘AACC’, where ‘A’ represents anti-clockwise and ‘C’ clockwise rotation of a single octahedron. This notation has been used previously to describe the complex sequence of tilt transitions seen in  $\text{NaNbO}_3$ .<sup>13</sup> Indeed, the tilt system seen here is identical in nature to that seen in the stable room temperature polymorph of  $\text{NaNbO}_3$ . In the original Glazer notation it can be described as a compound tilt

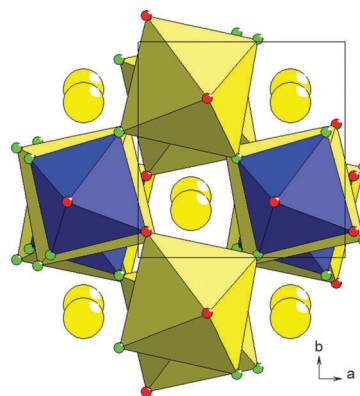


Fig. 4 Polyhedral view of the octahedral tilt scheme along the *c*-axis. Mo-centred octahedra blue, Na-centred octahedra yellow.



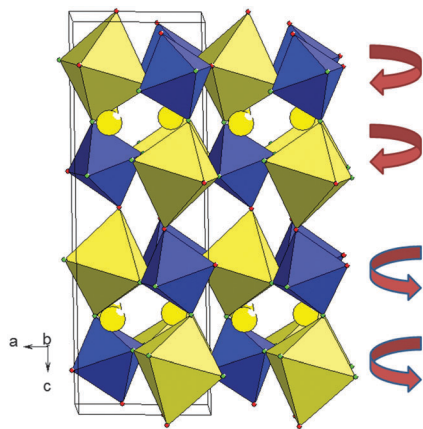


Fig. 5 Polyhedral view of the octahedral tilt scheme. Note the unusual AACC tilt scheme around the *c*-axis. Mo-centred octahedra blue, Na-centred octahedra yellow.

sequence  $a^-a^-b^+/a^-a^-b^-/a^-a^-b^+$ . This tilt system has been seen in only three perovskites previously:  $\text{NaNbO}_3$ ,<sup>14</sup>  $\text{AgNbO}_3$ ,<sup>15</sup> and  $\text{Ca}_{0.37}\text{Sr}_{0.63}\text{TiO}_3$ .<sup>16</sup>  $\text{KNaMoO}_2\text{F}_4$  displays no octahedral tilting, so it is clear that tilting occurs in the present case due to the tolerance factor effects normally associated with tilting in simpler perovskites. The specific and unusual nature of the tilting seen here, however, seems less easy to rationalise. The most common perovskite tilt system is  $a^-a^-b^+$ , as represented by the well-known 'GdFeO<sub>3</sub>-type' orthorhombic perovskite. This tilt system is stabilised by optimising A–X covalent interactions when the degree of tilting is relatively large.<sup>4</sup> In the present case the local tilt system around the Na(1) site is  $a^-a^-b^+$ , with in-phase tilting around *c*, whereas that around the vacant A-site has out-of-phase tilting around *c* ( $a^-a^-b^-$ , or approximately  $a^-a^-a^-$ ).

As there is no requirement in present case to satisfy bonding around the vacant A positions, it appears that the A-site layered ordering scheme co-operates with octahedral tilting to produce the unusual compound tilt system. This is supported by looking at the local bonding geometry around both the Na(1) site and the vacant A-site (Fig. 3). Here, the Na(1) site has the bonding typical of the  $a^-a^-b^+$  tilt system: viz. a staggered '4-long, 4-short' arrangement, whereas the vacant A-site (assuming the vacancy at the idealised position (1/4, 1/4, 1/2)) has a trigonal planar '3-short, 6-long' arrangement. Woodward<sup>4</sup> highlighted these local bonding environments as natural consequences of each tilting system: we note that the deviation of the Na(1) site from its ideal position (1/4, 1/4, 1/4) is relatively small ( $\sim 0.18$  Å), confirming that A-site bonding is optimised largely by tilts. Interestingly, the nature of the Na(1) displacement is analogous to that seen in antiferroelectric  $\text{NaNbO}_3$ ; viz. an 'antiferrodistortive' shift along the *b*-axis (Fig. 4). Perovskites with vacant A-sites, such as the fluorides  $\text{MF}_3$ ,<sup>17</sup> are known to favour 'out-of-phase' tilts ( $a^-a^-a^-$ ) over the more normal mixed tilt system  $a^-a^-b^+$ ; so too are the A-site deficient oxides e.g.  $\text{La}_{1/3}\text{NbO}_3$ , but the more complex tilt system seen here has not been reported in that series (perhaps because a more highly charged A-site cation is also known to favour  $a^-a^-a^-$  over  $a^-a^-b^+$ ).

In summary, exploratory hydrothermal synthesis has isolated a novel perovskite variant.  $\text{Na}_2\text{MoO}_{2-\delta}\text{F}_{4+\delta}$  exhibits several unusual structural features, including simultaneous atomic orderings at

all three of the sites in the  $\text{ABX}_3$  aristotype, a very rare octahedral tilt system and mixed valence. The distinct atomic orderings work cooperatively with the tilt scheme, in order to satisfy the bonding requirements around each site. The unique interplay of these different structural responses to compositional features suggests that further unusual perovskite variants might be discovered, by tailoring composition and reaction conditions within similar systems. Moreover, the observation of mixed valence prompts further study. In addition to the observation of slight O/F off-stoichiometry, the presence of an easily reducible cation,  $\text{Mo}^{6+}$ , together with vacant positions at the perovskite A-site suggest that intercalation chemistry will be possible to produce a wider range of  $\text{Mo}^{5+}$ -containing perovskites. As far as we are aware there are no well-characterised compounds of composition  $\text{A}_2\text{A}'\text{MoO}_2\text{F}_4$  (A, A' = alkali metal) for example, with filled A-sites; such compositions, exhibiting rock-salt type ordering of  $\text{Mo}^{5+}$  ( $S = 1/2$ ) on the perovskite B-site may give rise to interesting magnetic properties, as seen in some of the closely-related oxides, such as  $\text{Ba}_2\text{YMoO}_6$ .<sup>18</sup> Further, more systematic studies of the options for tailoring composition and mixed-valence, both in as-made samples and via subsequent electrochemical means will be carried out.

We acknowledge the University of St Andrews and the EPSRC (DTG: EP/K503162/1) for a studentship (to I.M.) and Mr Iain Patterson for experimental assistance. H.I. was supported by the Japan Society for the Promotion of Science, through the Program for Leading Graduate Schools (MERIT). The research data supporting this application can be accessed at <http://dx.doi.org/10.17630/1345bea9-2942-4404-9f8b-7635f1644a82>.

## Notes and references

§ An alternative and informative means of describing structural distortions in perovskites is by the use of distortion mode analysis. Such an analysis for the title compound, using the ISODISTORT software (B. J. Campbell, H. T. Stokes, D. E. Tanner and D. M. Hatch, *J. Appl. Crystallogr.*, 2006, **39**, 607) is given in the ESI†

- P. K. Davies, H. Wu, A. Y. Borisevich, I. E. Molodetsky and L. Farber, *Annu. Rev. Mater. Res.*, 2008, **38**, 369.
- G. King and P. M. Woodward, *J. Mater. Chem.*, 2010, **20**, 5785.
- A. M. Glazer, *Acta Crystallogr.*, 1972, **B28**, 3384.
- P. M. Woodward, *Acta Crystallogr.*, 1997, **B53**, 44.
- C. J. Howard and H. T. Stokes, *Acta Crystallogr.*, 1998, **B54**, 782.
- P. N. Iyer and A. J. Smith, *Acta Crystallogr.*, 1967, **23**, 740.
- P. A. Maggard, A. L. Kopf, C. L. Stern, K. R. Poeppelmeier, K. M. Ok and P. S. Halasyamani, *Inorg. Chem.*, 2002, **41**, 4852.
- D. W. Aldous and P. Lightfoot, *J. Fluorine Chem.*, 2012, **144**, 108.
- F. H. Aidoudi, C. Black, K. S. A. Arachchige, A. M. Z. Slawin, R. E. Morris and P. Lightfoot, *Dalton Trans.*, 2014, 568.
- I. N. Flerov, M. V. Gorev, A. Tressaud and N. M. Laptash, *Crystallogr. Rep.*, 2011, **56**, 9.
- R. A. F. Pinlac, C. L. Stern and K. R. Poeppelmeier, *Crystals*, 2011, **1**, 3.
- H. Shorafa, H. Ficicioglu, F. Tamadon, F. Girgsdies and K. Seppelt, *Inorg. Chem.*, 2010, **49**, 4263.
- M. D. Peel, S. E. Ashbrook and P. Lightfoot, *Inorg. Chem.*, 2012, **51**, 6876.
- A. C. Sakowski-Cowley, K. Lukaszewicz and H. D. Megaw, *Acta Crystallogr.*, 1969, **B25**, 851.
- J. Fábry, Z. Zikmund, A. Kania and V. Petricek, *Acta Crystallogr.*, 2000, **C56**, 916.
- C. J. Howard, R. L. Withers, K. S. Knight and Z. Zhang, *J. Phys.: Condens. Matter*, 2008, **20**, 135202.
- M. A. Hepworth, K. H. Jack, R. D. Peacock and G. J. Westland, *Acta Crystallogr.*, 1957, **10**, 63.
- M. A. de Vries, A. C. McLaughlin and J.-W. G. Bos, *Phys. Rev. Lett.*, 2010, **104**, 177202.

